

The First Year at LHC: Diffractive Physics

M. DEILE

CERN, Physics Department

ON BEHALF OF THE TOTEM COLLABORATION[†])

At the LHC, diffractive physics will be explored by the dedicated experiment TOTEM whose Technical Design Report has been approved in Summer 2004. The experimental programme will be carried out partly in TOTEM standalone mode for purely forward phenomena like elastic scattering, and partly in collaboration with CMS for processes requiring a full rapidity coverage. ATLAS and ALICE are interested in diffraction for a later stage.

This article presents the TOTEM/CMS running scenario for diffractive physics in the first year of LHC. We discuss which processes are within reach and with which statistics they can be measured.

Key words: diffraction,elastic scattering,total cross-section,luminosity, TOTEM, CMS

1 Introduction: Acceptance of TOTEM + CMS

At the interaction point 5 of the LHC the combined CMS and TOTEM detectors constitute a powerful instrumentation for studying diffractive physics. The TOTEM part contributes the forward trackers T1 and T2 inside CMS and a system of Roman Pot stations at distances of 147 m, 180 m and 220 m from the interaction point. The TOTEM detectors and their position w.r.t. CMS are described in [1] (see in particular Fig. 2 and 3 therein), and in more detail in the TOTEM TDR [2]. The two experiments will be able to take data together, with TOTEM acting technically as a subdetector of CMS with the capability to contribute to the level-1 trigger. The combined CMS+TOTEM experiment has a unique rapidity coverage together with an excellent acceptance for leading protons (Fig. 1). A part of the only coverage gap around $\eta = 8$ could be filled with an additional leading proton detector (e.g. a microstation) at a later time.

One ingredient for the determination of total cross-section and luminosity based on the optical theorem (see Section 3.1) is the measurement of the total elastic and inelastic rate. Minimum bias inelastic events produce particles distributed as shown in Fig. 2 (upper part). The coverage of T1, T2 overlaps sufficiently with the particle

[†]) V. Avati, V. Berardi, V. Boccone, M. Bozzo, A. Buzzo, M.G. Catanesi, S. Cuneo, C. Da Vià, M. Deile, K. Eggert, F. Ferro, E. Goussev, J.P. Guillaud, J. Hasi, F. Haug, R. Herzog, M. Järvinen, P. Jarron, J. Kalliopuska, K. Kurvinen, A. Kok, V. Kunderát, R. Lauhakangas, M. Lokajíček, D. Macina, M. Macrí, S. Minutoli, A. Morelli, P. Musico, M. Negri, H. Niewiadomski, E. Noschis, F. Oljemark, R. Orava, M. Oriunno, K. Österberg, V.G. Palmieri, A.-L. Perrot, E. Radicioni, R. Rudischer, G. Ruggiero, H. Saarikko, A. Santroni, G. Sanguinetti, G. Sette, W. Snoeys, A. Sobol, S. Tapprogge, A. Toppinen, A. Verdier, S. Watts and E. Wobst.

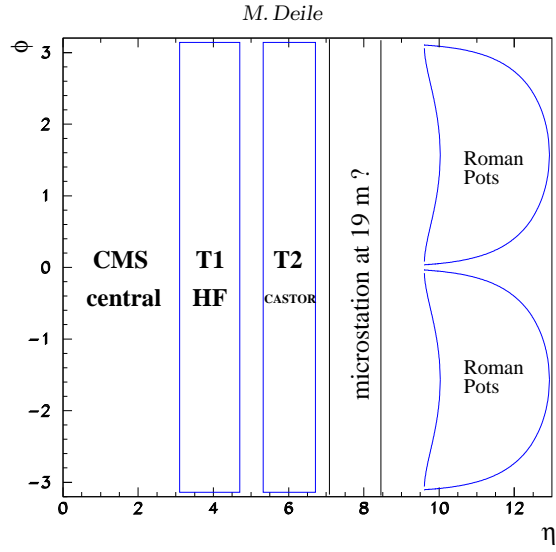


Fig. 1. Pseudorapidity-azimuth acceptance of the combined TOTEM and CMS experiments. The microstation at 19 m is not part of the present design.

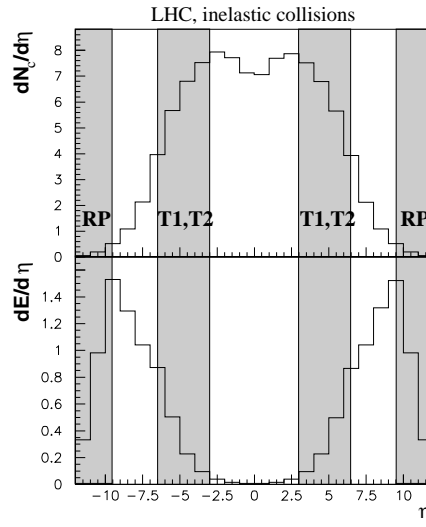


Fig. 2. Pseudorapidity distribution of the charged particle multiplicity (upper part) and of the energy flow (lower part) per generic inelastic event.

distribution, ensuring an efficiency of 99.9% for detecting minimum bias inelastic events. Elastic events on the other hand are well covered by the Roman Pots.

Considering that the energy flow in inelastic collisions is predominantly oriented in the forward direction (Fig. 2, lower part), the subdetectors T1, T2 and the HF and CASTOR calorimeters are valuable for studying forward showers as observed in cosmic ray physics.

2 The Running Scenarios

Running scenario	1	2	3	4
Physics	low $ t $ el., σ_{tot} , \mathcal{L} , soft diffr.	diffraction, \mathcal{L}	large $ t $ elastic	hard diffr.
β^* [m]	1540	1540	18	172
Number of bunches	43	156	2808	936 \div 2808
Protons per bunch	$0.3 \cdot 10^{11}$	$(0.6 \div 1.15) \cdot 10^{11}$	$1.15 \cdot 10^{11}$	$1.15 \cdot 10^{11}$
Transverse norm. emittance [$\mu\text{m rad}$]	1	$1 \div 3.75$	3.75	3.75
beam size at IP [μm]	454	$454 \div 880$	95	294
beam divergence at IP [μrad]	0.29	$0.29 \div 0.57$	5.28	1.7
$\frac{1}{2}$ crossing angle [μrad]	0	0	150	150
t_{min} [GeV^2] @ 220 m	$2 \cdot 10^{-3}$	$2 \cdot 10^{-3}$	1.3	$2 \cdot 10^{-2}$
t_{max} [GeV^2] @ 220 m	0.6	0.6	7	0.6
\mathcal{L} [$\text{cm}^{-2}\text{s}^{-1}$]	$1.6 \cdot 10^{28}$	$2.4 \cdot 10^{29}$	$3.6 \cdot 10^{32}$	$(1 \div 4) \cdot 10^{31}$

Table 1. TOTEM running scenarios.

The running scenarios for forward physics are listed in Table 1. For the precise measurement of proton scattering angles on the few μrad level a special beam optics scheme with $\beta^* = 1540$ m was developed. It is characterised by a small beam divergence in the interaction point ($0.29 \mu\text{rad}$) and a focal point in the Roman Pot station at 220 m for both the horizontal (x) and the vertical (y) track projections. In order to avoid parasitical bunch crossings downstream of the nominal interaction point due to the parallelism and large width (~ 0.4 mm) of the two beams, the number of bunches will be reduced from 2808 to initially 43 and later 156.

Scenario 1 will serve for measuring the elastic cross-section at low $|t|$ (Section 3.2), the total cross-section, the absolute luminosity (Section 3.1) and soft diffraction (Section 3.3). To minimize the emittance, these runs will be done with a smaller bunch population. Scenario 3 was introduced for measuring elastic scattering at large $|t|$. It offers a t -acceptance complementary to Scenario 1 and a higher

luminosity.

Higher luminosities for (semi-) hard diffraction (scenarios 2 and 4) can be reached by increasing the number of bunches and the bunch population. Some details of the optics for Scenario 4 are still under development.

TOTEM operation with normal LHC beam optics ($\beta^* = 0.5$ m) and $\mathcal{L} \sim 10^{33} \text{ cm}^{-2} \text{ s}^{-1}$ is under study but not yet part of the official programme. A common CMS+TOTEM letter of intent for diffractive physics is in preparation.

3 The Physics Programme

3.1 Total Cross-Section and Luminosity

Extrapolations of the total pp cross-section from existing measurements at $\sqrt{s} \leq 1.8$ TeV to the LHC CM energy of 14 TeV suffer from the conflicting TEVATRON measurements and cover a wide range, typically from 90 to 130 mb (see Fig. 1 in [1]). Cosmic ray experiments have provided direct measurements up to a few tens of TeV but with uncertainties on the 20% level. The TOTEM collaboration envisages a precision of about 1% using the Optical Theorem:

$$\sigma_{tot} = \frac{16\pi}{1 + \rho^2} \cdot \frac{dN_{el}/dt|_{t=0}}{N_{el} + N_{inel}}, \quad (1)$$

The extrapolation of the elastic cross-section to $t = 0$ suffers mainly from insufficient knowledge of the functional form (see Section 3.2) and from uncertainties in beam energy, detector alignment and crossing angle. The expected systematic error is about 0.5% whereas the statistical error is less than 0.1% for only 10 hours of running. The uncertainty of the total rate ($N_{el} + N_{inel}$) is given by trigger losses and beam-gas background [1]; it amounts to 0.8%. Taking also into account the uncertainty in $\rho = 0.12 \pm 0.02$ which enters only as a quadratic correction term, σ_{tot} can be measured with about 1% precision.

The same reasoning applies to the absolute luminosity measurement which is based on the same observables:

$$\mathcal{L} = \frac{1 + \rho^2}{16\pi} \cdot \frac{(N_{el} + N_{inel})^2}{dN_{el}/dt|_{t=0}} \quad (2)$$

Also here, a precision of the order 1% is expected. \mathcal{L} will be directly measured at TOTEM's running scenarios 1 and 2, i.e. at the relatively low luminosities of $1.6 \cdot 10^{28} \text{ cm}^{-2} \text{ s}^{-1}$ and $2.4 \cdot 10^{29} \text{ cm}^{-2} \text{ s}^{-1}$. In these two operating points the CMS luminosity monitors will be calibrated against TOTEM's absolute result, in order to be used later for relative measurements at higher luminosities.

A different approach is envisaged by the ATLAS collaboration [3]. It will be attempted to measure the differential cross-section of elastic scattering down to $-t < 6 \times 10^{-4} \text{ GeV}^2$ where the dominating Coulomb scattering provides the absolute scale. In practice, the measured event rate would be fitted to

$$\frac{dN}{dt} = \mathcal{L}\pi|f_C + f_N|^2 \approx \mathcal{L}\pi \left| -\frac{2\alpha}{|t|} + \frac{\sigma_{tot}}{4\pi} |i + \rho| e^{-b|t|/2} \right|^2 \quad (3)$$

with \mathcal{L} , σ_{tot} , ρ and b as free parameters.

3.2 Elastic Scattering

The differential cross-section $d\sigma/dt$ of elastic scattering according to the BSW model is shown in Fig. 3. Note that there is a rather wide range of predictions for $d\sigma/dt$ at LHC-typical centre-of-mass energies.

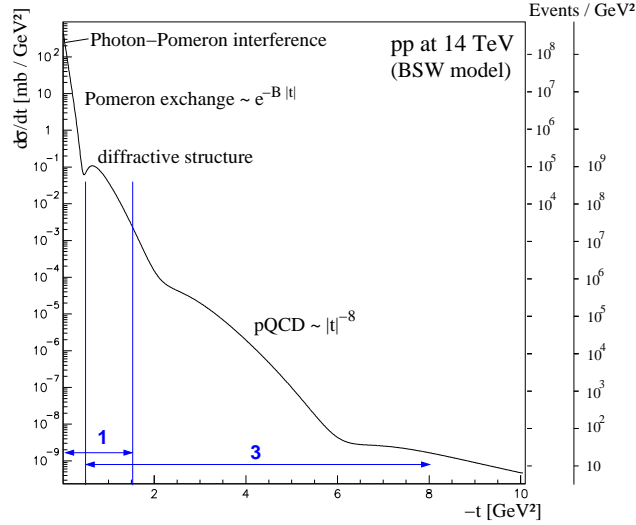


Fig. 3. Elastic cross-section predicted by the BSW model [4]. t is the four-momentum transfer, related to the scattering angle by $-t \approx p^2\theta^2$. The number of events on the right-hand scales correspond to integrated luminosities of 10^{33} and 10^{37} cm^{-2} (about 1 day with Scenarios 1 and 3).

TOTEM will cover the $|t|$ -range from 2×10^{-3} GeV^2 to 8 GeV^2 with its running scenarios 1 and 3 (Fig. 3). Since the t -acceptance for scenario 1 with its $\beta^* = 1540$ m optics ends around 1.5 GeV^2 (see also Fig. 10 in [1]) and since at higher $|t|$ more luminosity is needed, scenario 3 with a $\beta^* = 18$ m optics was created to extend the reach in $|t|$. The ranges accessible to the two scenarios overlap between 0.5 and 1.5 GeV^2 . Comfortable statistics can be collected in only 1 day of running with each of the scenarios (see right-hand scales in Fig. 3). At $|t| < 0.1 \text{ GeV}^2$ the statistics are sufficient for narrow bins of 10^{-3} GeV^2 width: at $2 \times 10^{-3} \text{ GeV}^2$ one will acquire 5×10^5 events per bin, and at 0.1 GeV^2 still 8×10^4 events per bin.

Assuming an elastic cross-section of 30 mb , about 5×10^7 events can be collected during one day at a luminosity of $1.6 \times 10^{28} \text{ cm}^{-2}\text{s}^{-1}$.

Access to the Coulomb and interference region at $|t| < 2 \times 10^{-3} \text{ GeV}^2$ will be attempted in two ways or a combination of them (see Fig. 4):

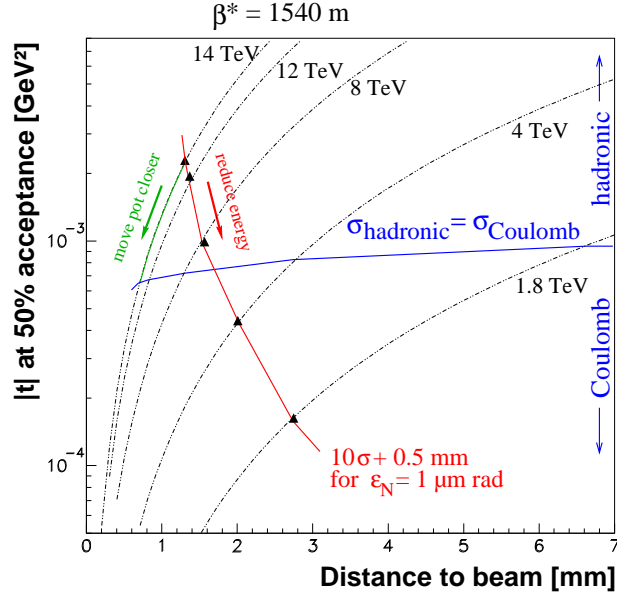


Fig. 4. t -value where 50% acceptance is reached, as a function of the detector distance from the beam centre, for different centre-of-mass energies. The nominal TOTEM operating point is at 14 TeV and a normalised emittance of $1 \mu\text{m rad}$ implying a detector-beam distance of $10\sigma + 0.5 \text{ mm} = 1.3 \text{ mm}$. To access the Coulomb region, either the distance between detector and beam or the energy has to be reduced.

- Move the Roman Pot detectors closer to the beam. This could be achieved by reducing the number of protons per bunch which would allow for a smaller emittance. The luminosity loss could be compensated by increasing the number of bunches. Suppose, the normalised emittance can be reduced to $\varepsilon_N = 0.5 \mu\text{m rad}$, and stable LHC operation allows the detectors to approach the beam to $10\sigma + \delta$ with $\delta = 0.1 \text{ mm}$. Then the $|t|$ -value with 50% acceptance would be given by

$$|t_{50}| = \frac{2p^2}{L_{\text{eff},y}^2} \left(10 \sqrt{\frac{\varepsilon_N \beta_y}{\gamma}} + \delta \right)^2 = 5.9 \times 10^{-4} \text{ GeV}^2, \quad (4)$$

where $p = 7 \text{ TeV}$ is the proton momentum, $L_{\text{eff},y} = 272 \text{ m}$ is the beam optics' effective length in the vertical plane, $\beta_y = 48 \text{ m}$ is the betatron function at the detector, and the relativistic γ is 7460.5.

- Run the LHC with a reduced centre-of-mass energy $\sqrt{s} = 2p \leq 6 \text{ TeV}$. According to (4), the reduction of $|t_{50}|$ with decreasing p due to the leading factor

p^2 is lessened by the $\frac{1}{\sqrt{\gamma}} \propto \frac{1}{\sqrt{p}}$ dependence of the beam width σ . The resulting effect behaves like $|t_{50}| \propto p^2 \left(\frac{C^2}{p} + 2\frac{C\gamma}{\sqrt{p}} + \delta^2 \right) = C^2 p + 2C\gamma p^{3/2} + \delta^2 p^2$.

3.3 Diffraction

3.3.1 Diffraction at $\beta^* = 1540$ m

The data taken during 1 day with scenario 1 contain not only 4.8×10^7 elastic events and 10^8 non-diffractive inelastic events, but also about 3.4×10^7 (mostly soft) diffractive events. Fig. 5 shows the basic classes of diffractive processes and the expected statistics with scenarios 1 and 2. The latter has the advantage of providing a 15 times higher luminosity which can serve for processes with small cross-section, such as Double Pomeron exchange or semi-hard phenomena.

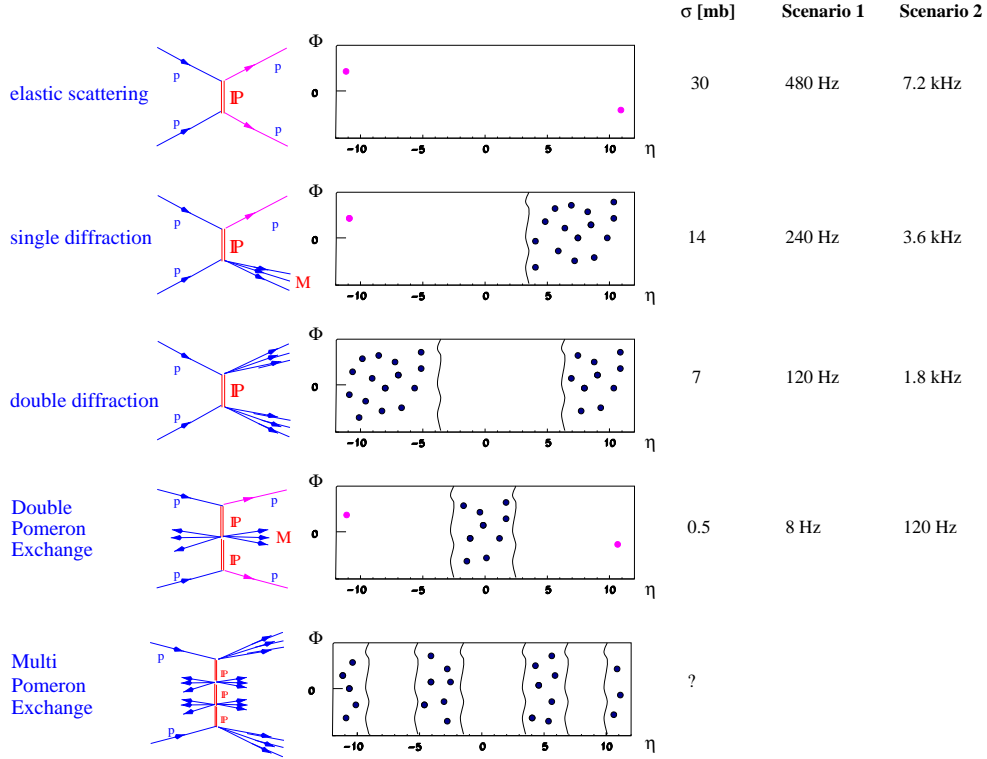


Fig. 5. Diffractive process classes (left) with their typical particle distributions in the pseudorapidity–azimuth plane (middle) and their expected event rates with the two high- β^* running scenarios (right). Scenario 1 has $\mathcal{L} = 1.6 \cdot 10^{28} \text{ cm}^{-2}\text{s}^{-1}$ and scenario 2 has $\mathcal{L} = 2.4 \cdot 10^{29} \text{ cm}^{-2}\text{s}^{-1}$.

Note that the estimates of diffractive cross-sections are based on rather uncertain extrapolations from lower energies to LHC conditions. The simultaneous observation of rapidity gaps $\Delta\eta$ and the momentum loss $\xi \equiv \Delta p/p$ of surviving protons will allow to test the relationship $\Delta\eta = -\ln \xi$, valid for pure colour singlet exchange. It is still unknown with which probability the rapidity gaps will “survive” at LHC energies, i.e. not be filled by hadronisation from higher-order soft rescattering processes.

The great advantage of the scenarios at $\beta^* = 1540$ m is the very good acceptance in momentum transfer t and momentum loss $\xi \equiv \Delta p/p$ (Fig. 6). For $|t| > 0.002$ all protons are detected independent of ξ . Assuming a differential cross-section

$$\frac{d\sigma}{d\xi dt} \propto \frac{1}{\xi} e^{-B|t|} \quad (5)$$

with $B = 5.6 \text{ GeV}^{-2}$, the total acceptance (integrated over t and ξ) is about 95 %.

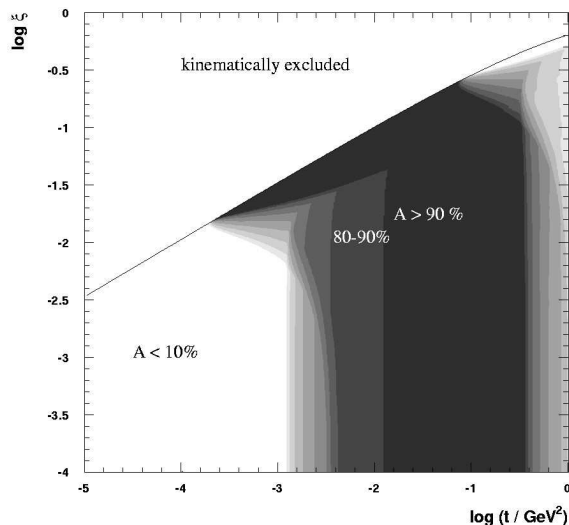


Fig. 6. Acceptance for diffractive protons with the 1540 m optics in the RP station at 220 m.

The ξ resolution using the RP stations at 147 m and 220 m with the dipole D2 in between is about 5×10^{-3} .

3.3.2 Diffraction at Intermediate β^*

For double-pomeron exchange and hard diffractive processes with their lower cross-sections, scenario 4 with a luminosity of the order $10^{31} \text{ cm}^{-2}\text{s}^{-1}$ will be advantageous. Although some details of that scenario are still under study, the accep-

tance in t and ξ is expected to be about 86 %. For the ξ -resolution a level of $\lesssim 10^{-3}$ will be attempted, i.e. an improvement of a factor 5 w.r.t. the $\beta^* = 1540$ m optics.

Double Pomeron Exchange (DPE)

Figure 7 shows the differential cross-section of double-pomeron processes extrapolated to LHC energies. The event numbers per day (right-hand scales) show by extrapolation that diffractive systems with masses up to about 2 TeV are well within reach.

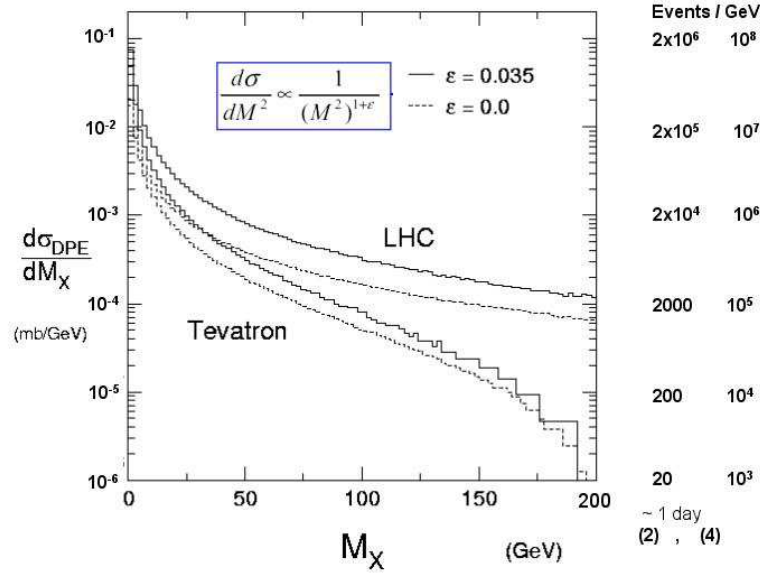


Fig. 7. Differential cross-section of double-pomeron processes and the expected number of events per day for scenarios 2 ($\mathcal{L} = 2.4 \cdot 10^{29} \text{ cm}^{-2} \text{ s}^{-1}$) and 4 ($\mathcal{L} \sim 10^{31} \text{ cm}^{-2} \text{ s}^{-1}$). The continuous and dashed curves represent two models with different Pomeron trajectories $\alpha(t) = 1 + \varepsilon + \alpha' t$.

A particularly interesting class of double-pomeron events is exclusive central production. It is characterised by a clean signature of two surviving protons, two rapidity gaps and only a single particle (or a dijet) in the diffractive system. Due to the exchange of colour-singlets (having the quantum numbers of the vacuum), the states produced in the centre must obey selection rules on spin J , parity P and charge conjugation C [5]:

$$J^P = 0^+, 2^+, 4^+; J_z = 0; C = +1 \tag{6}$$

(in the limit of $t = 0$). The $J_z = 0$ rule strongly suppresses $gg \rightarrow q\bar{q}$ background because of helicity conservation (this background would totally vanish for massless quarks).

Some examples for exclusive production are given in Table 2.

Diffractive system	σ	Decay channel	BR	Rate at $\mathcal{L} [\text{cm}^{-2}\text{s}^{-1}] =$		
				2.4×10^{29}	10^{31}	10^{33}
χ_{c0} (3.4 GeV)	$3 \mu\text{b}$	$\gamma J/\psi \rightarrow \gamma \mu^+ \mu^-$ $\pi^+ \pi^- K^+ K^-$	6×10^{-4} 0.018	1.6 / h 47 / h	65 / h 1944 / h	6480 / h 54 / s
χ_{b0} (9.9 GeV)	4 nb	$\gamma Y \rightarrow \gamma \mu^+ \mu^-$	$\leq 10^{-3}$	≤ 0.07 / d	≤ 3 / d	≤ 300 / d
H (SM) (120 GeV)	3 fb	bb	0.68	0.02 / y	1 / y	100 / y

Table 2. Examples of exclusive DPE processes ($p + p \rightarrow p + X + p$). The rates do not account for any acceptance or analysis cuts. For cross-sections see e.g. [6, 7].

The χ_c resonance may be within reach. The χ_b resonance is more uncertain because the branching ratios of its decays are not known. Detecting a 120 GeV Higgs requires luminosities higher than the ones of the running scenarios established so far. For this purpose, new scenarios for standard LHC optics ($\beta^* = 0.5$ m) and luminosities ($\mathcal{L} \sim 10^{33} \text{ cm}^{-2}\text{s}^{-1}$) are being developed for a later stage. These ideas also involve additional RP stations in the cryogenic LHC region (at 308 m, 338 m and 420 m from the IP) in order to achieve an adequate ξ acceptance.

Hard Diffraction

If a diffractive event involves a hard subprocess, the diffractive system (‘M’ in Fig. 5) will contain jets. As an example, Table 3 gives the cross-sections and production rates for dijets in DPE.

DPE Dijets ($E_T > 10$ GeV)	σ	Rate at $\mathcal{L} [\text{cm}^{-2}\text{s}^{-1}] =$	
		2.4×10^{29}	10^{31}
inclusive	$1 \mu\text{b}$	864 / h	10 / s
exclusive	7 nb	6 / h	252 / h

Table 3. Cross-sections and rates for inclusive and exclusive dijets production by double-pomeron exchange [6, 8].

4 Conclusions

A menu for elastic and diffractive physics in the first year of LHC has been outlined. Starting with several runs of about 1 day with the dedicated $\beta^* = 1540$ m and 18 m beam optics, a data sample containing about 10^8 minimum bias events, 4.8×10^7 elastic events and 3.4×10^7 diffractive events will be collected. These data will serve for the measurement of the total cross-section and the luminosity

with about 1% precision. The elastic differential cross-section will be studied in a momentum transfer range from 10^{-3} GeV^2 to 8 GeV^2 . In addition, attempts will be made to reach the Coulomb/nuclear interference region at $t \lesssim 6 \times 10^{-4} \text{ GeV}^2$ by running LHC at a lower energy $\sqrt{s} \lesssim 6 \text{ TeV}$ or with reduced emittances.

The data already recorded at that stage will also allow studies of soft diffraction. Expected are 2.4×10^7 single diffractive, 1.2×10^7 double diffractive and 0.1×10^7 double Pomeron events.

To make semi-hard diffractive processes (involving transverse momenta $> 10 \text{ GeV}$) accessible, the number of bunches and the bunch population will be increased to yield a 15 times higher luminosity, while keeping the optics unchanged.

For hard diffraction and rare DPE phenomena an additional optics configuration with $\beta^* = 170 \text{ m}$ and a luminosity of $(1 \div 4) \times 10^{31} \text{ cm}^{-2}\text{s}^{-1}$ is under development.

In the farther future there will also be a diffractive programme for standard LHC running conditions with the $\beta^* = 0.5 \text{ m}$ optics and luminosities $\sim 10^{33} \text{ cm}^{-2}\text{s}^{-1}$, possibly giving access to very rare processes like exclusive Higgs production.

References

- [1] F. Ferro et al.: Status of TOTEM, these proceedings.
- [2] TOTEM: Technical Design Report, CERN-LHCC-2004-002
- [3] ATLAS Forward Detectors for Luminosity Measurement and Monitoring, Letter of Intent, CERN/LHCC/2004-010.
- [4] C. Bourelly et al., *Eur. Phys. J.* **C28** (2003) 97.
- [5] V.A. Khoze, A.D. Martin, M.G. Ryskin, *Eur. Phys. J.* C19 (2001) 477.
- [6] V.A. Khoze, A.D. Martin, M.G. Ryskin, *Eur. Phys. J.* C23 (2002) 311.
- [7] V.A. Khoze, A.D. Martin, M.G. Ryskin, W.J. Stirling, *Eur. Phys. J.* C35 (2004) 211-220.
- [8] V.A. Petrov, R.A. Ryutin, *JHEP* 0408 (2004) 013.